ELSEVIER

PII: S0032-3861(98)00071-8

Polymer Vol. 39 No. 26, pp. 7079–7087, 1998

0032-3861/98/$ - see front matter

Structure–property relationships of polyimides: a molecular simulation approach

Jin Woo Kang[a], Kyoungsei Choi[a], Won Ho Jo[a,*] and Shaw Ling Hsu[b]
[a]*Department of Fiber and Polymer Science, Seoul National University, Seoul 151-742, South Korea*
[b]*Department of Polymer Science and Engineering, University of Massachusetts, Amherst, MA 01003, USA*
(Received 25 November 1997; accepted 9 January 1998)

Chain flexibility and mechanical properties of four polyimides with different chemical structures are simulated by molecular dynamics and molecular mechanics techniques to establish some structure–property relationships. The oxygen linkage in the diamine moiety of a polyimide gives the highest flexibility whereas the sulfonyl linkage imparts the lowest flexibility to the polymer chain. A more flexible polyimide has smaller characteristic ratio, lower solubility parameter, lower elastic modulus, and larger yield strain. These simulated values show good agreement with experimental data. © 1998 Elsevier Science Ltd. All rights reserved.

(Keywords: polyimide; structure–property; molecular simulation)

INTRODUCTION

In the past decade, atomistic modelling techniques have been applied to polymeric materials in an attempt to predict their macroscopic properties (e.g. modulus, yield behaviour, thermal expansion coefficient) as well as microscopic properties (e.g. configuration, conformation, chain orientation), although these techniques have some inherent limitations of time and/or space scale. Earlier, Theodorou and Suter[1,2] developed an atomistic modelling technique to generate a model of a well-relaxed amorphous polypropylene sample and to predict its elastic constants using the stiffness matrix. Later, several other researchers calculated the mechanical properties of various polymers such as polyethylene[3], polysulfone[4], polystyrene[5], polycarbonate[6,7] and polybenzoxazole[8], using atomistic modelling techniques.

Generally, polyimides have good thermal stability, excellent mechanical properties, high softening temperatures and good electrical properties. However, their properties strongly depend on their chemical structure, i.e. a slight modification of the chemical structure may often result in a significant change in mechanical properties. Thus development of structure–property relationships for polyimides may provide a guideline for designing polyimides having desirable end-use properties.

In this study, the mechanical properties of four polyimides with different chemical structures are calculated using atomistic modelling techniques, and the results are compared with experimental data. An attempt is made to establish structure–property relationships for polyimides by relating the chemical structures of individual polyimides to their conformational and mechanical properties.

* To whom correspondence should be addressed

MODEL AND SIMULATIONS

The chemical structures of the repeat units of the four polyimide models used in this study are shown in *Figure 1*. The four polyimides can be synthesized from 3,3′-4,4′-benzophenone tetracarboxylic dianhydride (BTDA) and corresponding diamine, i.e. *p*,*p*′-carbonyldianiline (CDA), *p*,*p*′-oxydianiline (ODA), *p*,*p*′-sulfonyl dianiline (SDA) and *p*,*p*′-methylene dianiline (MDA). For convenience, the model polyimides are denoted PI-1 for BTDA-CDA, PI-2 for BTDA-ODA, PI-3 for BTDA-SDA and PI-4 for BTDA-MDA. Four virtual bonds (1, 4, 5 and 8 in *Figure 1*) and four covalent bonds (2, 3, 6 and 7 in *Figure 1*) are used to trace the chain through the large repeat unit. Each polyimide simulated consists of 15 repeating units so that the total numbers of atoms are 782, 767, 797 and 797, respectively. The system size of 15 repeat units is not enough to represent conformations of a real polymer chain. However, previous workers[4–8] have reported reasonable results when they used 10 to 15 repeat units for simulation. Periodic boundary conditions were imposed and an initial density of 1.20 g/cm^3 was used to simulate the bulk amorphous state. Six model structures were generated for each polyimide using the method of Fan and Hsu[9]. Dihedral angles along the chain backbone of each polyimide were randomly assigned using a Monte Carlo method, and then this initial structure was optimized by a molecular mechanics technique. Because this optimized structure might, however, be still in a local energy minimum state, this was relaxed through NVT molecular dynamics for 200 ps at 1000 K, followed by several cycles of molecular mechanics and NPT molecular dynamics for 200 ps at room temperature under the pressure of 10^5 Pa. Finally a full optimization for cell parameters and atomic coordinates was performed by molecular mechanics, and the equilibrium density of each structure was obtained.

The commercial software *Cerius*^{2} from Molecular Simulation Inc. was used and the Dreiding force field[10]

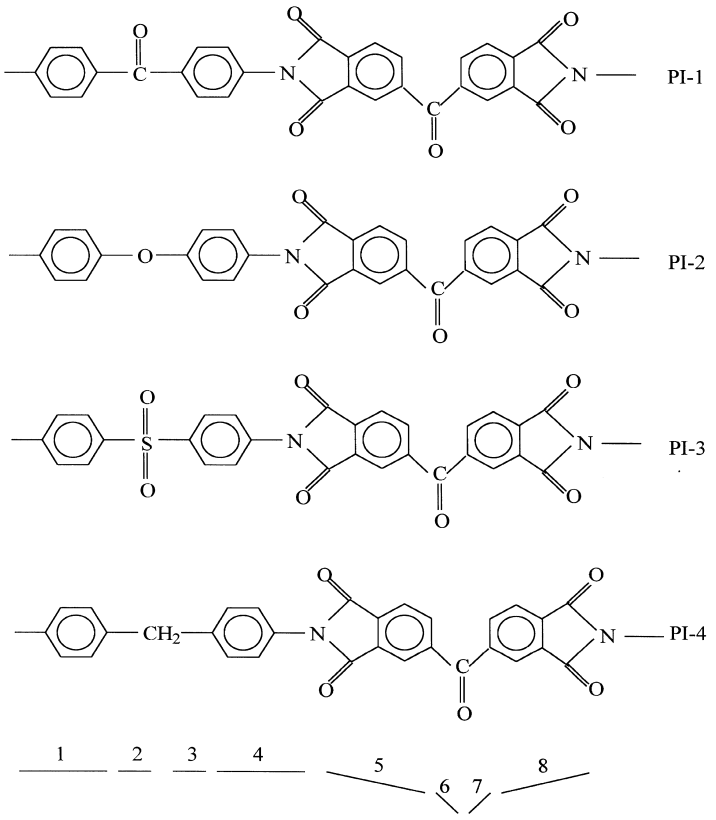

Figure 1 The repeat units and the definition of virtual bonds of polyimides: (a) PI-1 (BTDA-CDA), (b) PI-2 (BTDA-ODA), (c) PI-3 (BTDA-SDA), and (d) PI-4 (BTDA-MDA)

was adopted, in this study, to calculate potential energies between atoms. The potential energy is given as the sum of the following terms:

$$E = E_l + E_\theta + E_\phi + E_{inv} + E_{vdW} + E_{Coul} \quad (1)$$

where E_l, E_θ and E_ϕ are the bond stretching, valence angle bending, and torsion terms, respectively, E_{inv} is the improper out-of-plane interaction, and E_{vdW} and E_{Coul} are the non-bonded van der Waals and Coulomb interactions. The Ewald summation method was used to calculate the nonbond interaction energy.

RESULTS AND DISCUSSION

Validation of simulations

The use of the Dreiding force field for our systems was validated by the following method. The monomeric unit of each polyimide was packed into a crystalline cubic cell, and then its atomic coordinates and cell parameters were optimized. *Figure 2* shows the mean bond lengths and angles of linkage groups in the polyimides obtained from X-ray experimental data[11]. The simulated crystal data are listed in *Table 1* and compared with the experimental data. A good agreement between simulated and experimental data validates the use of the force field for our systems. Recently, it was also reported that the structure and energetics of a thermoplastic polyimide were successfully simulated by use of the Dreiding force field[12].

Six model structures for each polyimide were generated through several cycles of energy minimization and molecular dynamics, followed by a full optimization of cell parameters and atomic coordinates. The properties of each polyimide were then ensemble averaged for more reliable

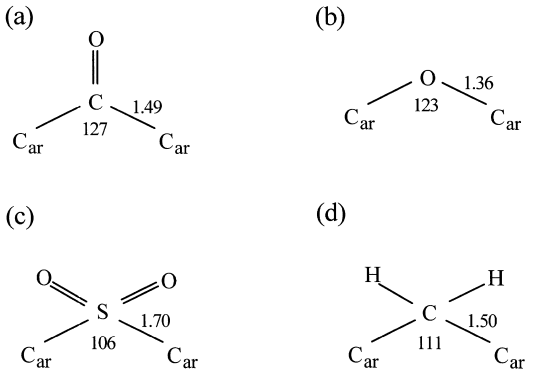

Figure 2 Mean bond lengths (Å) and angles (degrees) of linkage groups in polyimides obtained from X-ray experiments[11]

results. The averaged cell parameters of each polyimide are listed in *Table 2*. The deviations from a cube in cell lengths and angles are so small that the model structures are considered to represent an isotropic state. Simulated densities are listed in *Table 3* and compared with

Table 1 Mean bond lengths and angles in linkage groups of polyimides from simulation and experiment[11]

Polymers	Bond length (Å)		Bond angle (degrees)	
	Simulation	Experiment	Simulation	Experiment
PI-1	1.50 ± 0.04	1.49	128.6 ± 0.9	127
PI-2	1.36 ± 0.06	1.36	122.5 ± 0.7	123
PI-3	1.72 ± 0.11	1.70	108.1 ± 1.2	106
PI-4	1.50 ± 0.08	1.50	109.8 ± 0.7	111

Table 2 Averaged cell parameters of the model polyimides

Polymers	Cell parameters					
	a (Å)	*b* (Å)	*c* (Å)	α (degrees)	β (degrees)	γ (degrees)
PI-1	22.14 ± 0.86	21.72 ± 0.91	20.63 ± 0.59	90.93 ± 1.90	88.36 ± 3.08	89.84 ± 2.77
PI-2	21.32 ± 0.69	20.95 ± 0.46	21.67 ± 0.82	88.49 ± 3.71	90.54 ± 1.67	89.25 ± 2.44
PI-3	21.59 ± 0.73	21.87 ± 0.50	21.95 ± 0.64	89.56 ± 2.38	89.05 ± 1.85	91.03 ± 2.11
PI-4	20.79 ± 0.38	21.47 ± 0.72	21.31 ± 0.75	89.45 ± 3.41	90.87 ± 2.90	90.28 ± 3.69

experimental data. The simulated densities are *ca*. 5% lower than the experimental ones. Such lower values of densities from simulation have been reported for several other polymers[4,7,8]. This may be partly due to the use of a short chain (15 repeat units in this simulation) for simulation, because it is known that the simulated density is sensitive to the system size. Nevertheless, agreement between simulated density and the experimental one within 5% error may validate the van der Waals term in the force field used in this study. *Table 4* lists the average values of all components of the internal stress tensors. All these values are close to zero, indicating that the polymer structures generated are fully relaxed and in the equilibrium state.

Radial distribution functions were calculated to verify that the simulated structures have an amorphous nature. This function is defined as a probability of finding a pair of all kinds of atoms in the system at a distance *r* apart relative to the probability expected for a completely random distribution at the same density. The averaged radial distribution functions of the four model polyimides are shown in *Figure 3*. All the correlation functions show two sharp peaks at about 1.1 and 1.5 Å. The former and latter peaks are associated with C-H bonds and C-C (or C = C) bonds, respectively. Peaks at distances of 2 Å–4 Å are generally due to nonbonded atoms separated by two (1–3), three (1–4) and four (1–5) bonds on the connected chain. Another feature of note is the absence of sharp peaks at distances greater than 4 Å. This fact clearly demonstrates the amorphous nature of the simulated polyimides, i.e. complete absence of long-range order.

Conformational properties

Analysis of conformational behaviour provides useful information on the local structure, chain flexibility, and average dimensions of polymers. Since this behaviour is influenced by even a slight modification of polymer structure, we may expect that the four model structures for polyimides show significantly different properties. Conformational grid searches allow us to vary simultaneously the torsional angles of successive bonds and to plot the total energy against each pair of rotational angles. In the grid scan method, the potential energy is calculated whenever a specific torsional angle is varied over a grid of an equally spaced value. When the rotations of two successive bonds are considered, the torsional angle of the first bond is fixed at a given value and then the potential energies are calculated while the torsional angle of the second bond is varied. Subsequently, the torsional angle of the first bond is set to another value and the potential energies are then calculated while the second bond angle is varied, and so on. For the conformational grid search, only one repeat unit of polyimides is considered, since we are only concerned with energies associated with torsional rotations of particular bonds. In this study, the torsional angles about the bonds 2 and 3 in *Figure 1* are primarily concerned, because the only difference between the four polyimides is rotations about these two bonds. During a conformational search, the chain conformations besides the concerned bonds are fixed. Potential energy contour maps of the four polyimides are shown in *Figure 4*, where energy contour lines are drawn every 1 kcal/mol and local energy minima are marked by + signs. As shown in *Figure 4*a, two synchronous motions by two rotations are observed in PI-1. For example, the rotational angle ϕ_2 changes from 0° to −70° or from 0° to 120°, while the angle ϕ_3 changes from −150° to −40°. The energy barriers of these two motions are about 3.0 kcal/mol and 8.0 kcal/mol. Thus the first type of motion is energetically preferred, and thereby dominantly occurs in short time dynamics or under small deformations. As a result, if one angle of local energy minimum is given, the other angle is automatically determined because only one path is probable. The potential energy contour map of PI-2 is shown in *Figure 4*b, where the energy barrier between two minima is about 2.0 kcal/mol or 8.0 kcal/mol. Moreover, various types of cooperative motions may be allowed. The relatively low energy barriers and more allowed motions may impart chain flexibility to this

Table 3 Averaged densities of the model polyimides

	Simulated density (g/cm^3)	Experimental density (g/cm^3)
PI-1	1.25 ± 0.03	1.33[a]
PI-2	1.25 ± 0.02	1.30[b]
PI-3	1.28 ± 0.03	1.38[c]
PI-4	1.27 ± 0.03	1.33[b]

[a]Taken from [16]
[b]Taken from [11]
[c]Taken from [15]

Table 4 Averaged internal stress components (MPa) of the model polyimides

Polymers	Stress components					
	xx	*yy*	*zz*	*xy*	*yz*	*zx*
PI-1	−0.16 ± 0.25	0.33 ± 0.39	0.23 ± 0.71	0.17 ± 0.32	−0.25 ± 0.56	−0.05 ± 0.47
PI-2	0.38 ± 0.54	0.21 ± 0.37	0.47 ± 0.49	−0.14 ± 0.63	−0.22 ± 0.85	−0.27 ± 0.38
PI-3	0.43 ± 0.41	−0.37 ± 0.59	0.25 ± 0.69	−0.56 ± 0.60	0.28 ± 0.42	−0.13 ± 0.39
PI-4	0.29 ± 0.48	−0.25 ± 0.66	0.62 ± 0.43	−0.41 ± 0.65	−0.04 ± 0.51	−0.18 ± 0.40

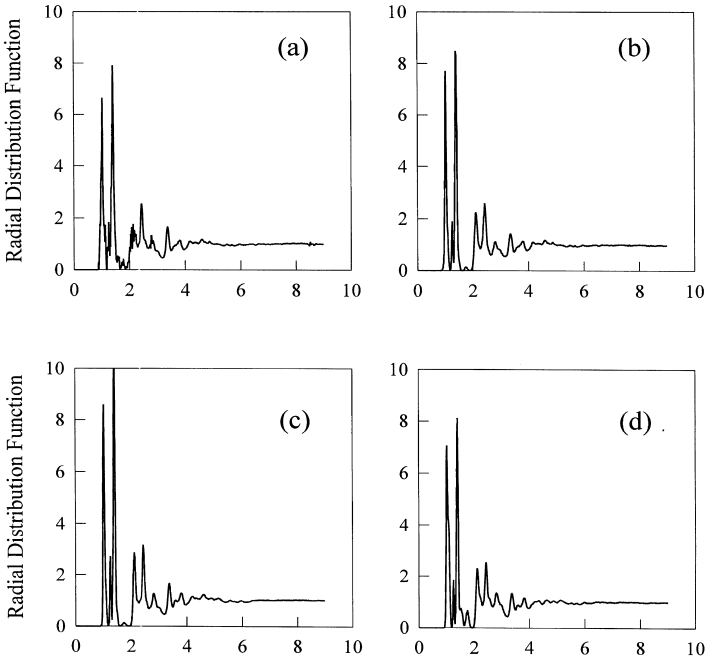

Figure 3 Averaged radial distribution functions for model polyimides: (a) PI-1, (b) PI-2, (c) PI-3, (d) PI-4

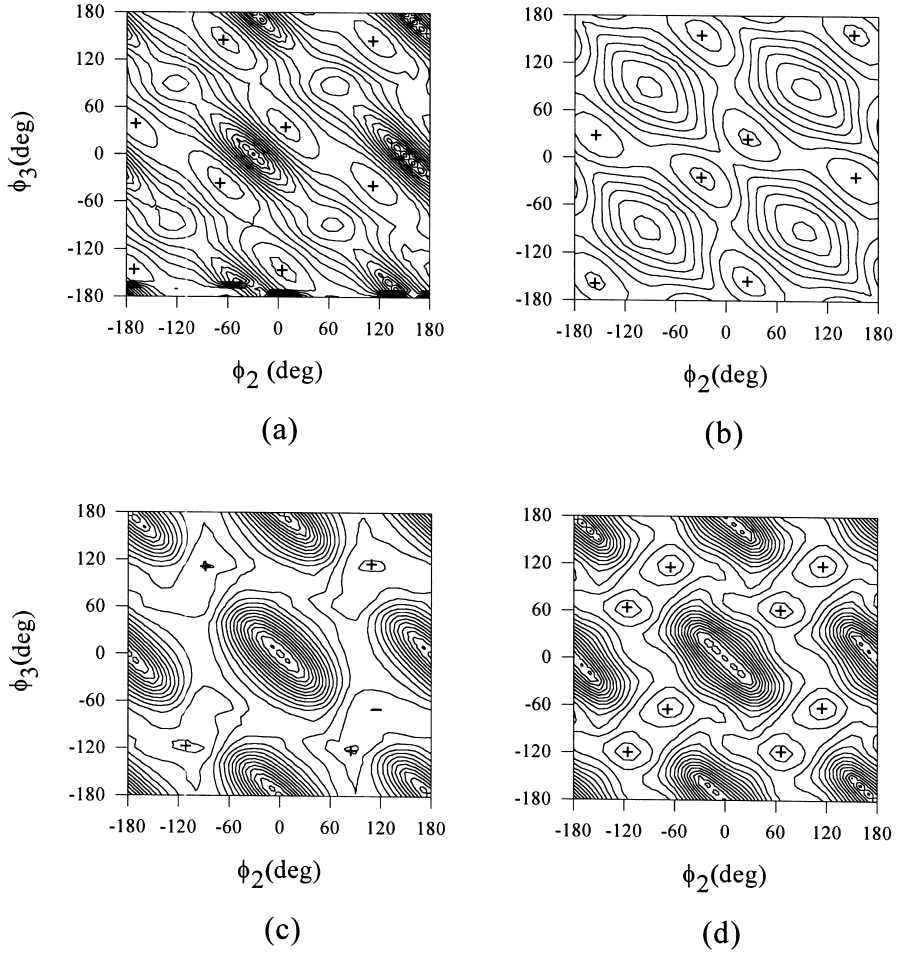

Figure 4 Potential energy contour maps as a function of ϕ_2 and ϕ_3: (a) PI-1, (b) PI-2, (c) PI-3, and (d) PI-4. Energy difference between contour lines is 1 kcal/mol

polymer. In contrast to PI-2, the energy barrier between two minima for PI-3 is about 14.0 kcal/mol as shown in *Figure 4*c and the number of allowed motions is rather limited. Thus it is expected that PI-3 is less flexible compared with PI-1 and PI-2. In summary, it may be concluded from conformational analysis that PI-2 is the most flexible due to a lower energy barrier and more freedom of conformational motions whereas PI-3 is the most rigid.

The characteristic ratio of a polymer chain is often used as a quantitative measure of chain flexibility. This ratio is defined as the ratio of the square of the end-to-end distance of a given polymer to that of the equivalent freely jointed chain with the same bond lengths. Thus the characteristic ratio is equal to

$$C_n = \langle r^2 \rangle / \sum_{i=1}^{n} l_i^2 \tag{2}$$

where $\langle r^2 \rangle$ is the mean-squared end-to-end distance, n is the number of bonds, and l_i is the bond length of each bond. The characteristic ratio may be calculated by directly measuring the squared chain end-to-end distances and dividing the average by $\sum l_i^2$. However, when the number of model chains is small , e.g. six as in our case, this method may lead to a sizable statistical error. Another way to calculate the chain end-to-end distance is the use of the transformation matrix[13,14], whose components are composed of statistical averages of the bond lengths, bond angles, and dihedral angles. In this method, the statistical error can be reduced because the sample size is related to the total number of bonds used for simulation. In this study, therefore, the latter method was used. As shown in *Figure 1*, one repeating unit has 8 bonds (4 covalent bonds and 4 virtual bonds), and thus the number of bonds of one model chain is 120 because each polymer has 15 repeating units. Since six models of each polymer are used for an ensemble average, the total number of bonds for each polymer simulated becomes 720. Therefore, the result from the transformation matrix method should undoubtedly be more reliable than the direct measurement method. The average bond lengths, the average sines and cosines of the bond angles, and the average sines and cosines of torsional angles are listed in *Tables 5–7*, respectively. The mean squared end-to-end distance of each polymer can be calculated using these data through the following relation[13,14]:

$$\langle r^2 \rangle = \langle \mathbf{G}_1 \rangle \langle \mathbf{G}_2 \rangle \langle \mathbf{G}_3 \rangle \cdots \langle \mathbf{G}_n \rangle \tag{3}$$

where the $\mathbf{G}_i$s are the so-called generator matrices, with

$$\mathbf{G}_1 = \begin{pmatrix} 1 & 2\mathbf{I}_1^{\mathrm{T}}\mathbf{T}_1 & \mathbf{I}_1^2 \end{pmatrix} \tag{4}$$

$$\mathbf{G}_i = \begin{pmatrix} 1 & 2\mathbf{I}_i^{\mathrm{T}}\mathbf{T}_i & l_i^2 \\ 0 & \mathbf{T}_i & \mathbf{I}_i \\ 0 & 0 & 1 \end{pmatrix} \quad 1 < i < n \tag{5}$$

$$\mathbf{G}_n = \begin{pmatrix} l_n^2 \\ \mathbf{I}_n \\ 1 \end{pmatrix}. \tag{6}$$

In the above equations, the matrices $\mathbf{T}_i$ are transformation

Table 5 Averaged lengths (Å) of covalent and virtual bonds in the model polyimides

Polymers	Bond i			
	1,4	2,3	5,8	6,7
PI-1	4.25 ± 0.05	1.42 ± 0.02	4.65 ± 0.07	1.42 ± 0.01
PI-2	4.21 ± 0.03	1.36 ± 0.01	4.63 ± 0.02	1.42 ± 0.01
PI-3	4.21 ± 0.04	1.74 ± 0.01	4.63 ± 0.02	1.42 ± 0.01
PI-4	4.23 ± 0.02	1.49 ± 0.01	4.63 ± 0.03	1.41 ± 0.01

Table 6 Averaged sines and cosines of the angles between virtual bonds i and $i + 1$

Polymers		Bond i				
		1,3	2	4,8	5,7	6
$\langle \sin\theta_i \rangle$	PI-1	0.242 ± 0.181	0.751 ± 0.066	0.295 ± 0.099	0.399 ± 0.037	0.809 ± 0.027
	PI-2	0.147 ± 0.088	0.775 ± 0.067	0.213 ± 0.085	0.378 ± 0.034	0.831 ± 0.017
	PI-3	0.132 ± 0.090	0.896 ± 0.036	0.258 ± 0.117	0.370 ± 0.038	0.810 ± 0.023
	PI-4	0.072 ± 0.056	0.903 ± 0.029	0.248 ± 0.083	0.378 ± 0.038	0.825 ± 0.020
$\langle \cos\theta_i \rangle$	PI-1	−0.951 ± 0.081	−0.619 ± 0.075	−0.950 ± 0.032	−0.916 ± 0.016	−0.586 ± 0.037
	PI-2	−0.985 ± 0.018	−0.505 ± 0.082	−0.973 ± 0.023	−0.925 ± 0.014	−0.556 ± 0.027
	PI-3	−0.987 ± 0.018	−0.476 ± 0.084	−0.959 ± 0.038	−0.928 ± 0.015	−0.585 ± 0.033
	PI-4	−0.996 ± 0.006	−0.527 ± 0.056	−0.965 ± 0.024	−0.925 ± 0.016	−0.565 ± 0.029

Table 7 Averaged cosines of the torsional angles at virtual bonds i in the model polyimides

Polymers	Bond i			
	1,4	2,3	5,8	6,7
PI-1	0.682 ± 0.073	−0.120 ± 0.118	0.617 ± 0.141	−0.061 ± 0.144
PI-2	0.564 ± 0.155	−0.039 ± 0.116	0.799 ± 0.115	−0.056 ± 0.161
PI-3	0.448 ± 0.164	−0.164 ± 0.126	0.712 ± 0.127	−0.068 ± 0.167
PI-4	0.258 ± 0.207	0.014 ± 0.181	0.721 ± 0.112	0.047 ± 0.174

matrices of the form

$$\langle \mathbf{T}_i \rangle = \begin{pmatrix} -\langle \cos\theta_i \rangle & \langle \sin\theta_i \rangle & 0 \\ -\langle \sin\theta_i \rangle\langle \cos\phi_i \rangle & -\langle \cos\theta_i \rangle\langle \cos\phi_i \rangle & 0 \\ 0 & 0 & \langle \cos\phi_i \rangle \end{pmatrix} \tag{7}$$

where θ_i is the angle between bonds i and $i+1$ and ϕ_i is the torsional angle of bond i. The use of equation (3) implicitly assumes that all bonds are independent, although bonds 2 and 3 as well as bonds 6 and 7 may be interdependent as seen from the potential energy contour maps. However, it has been reported that the interdependency between virtual bonds does not significantly affect the value of the characteristic ratio[13]. *Figure 5* shows the characteristic ratios of the four polyimides as a function of the number of repeating units. PI-3 has the largest characteristic ratio and PI-2 has the lowest. It is clearly seen that PI-2 is the most flexible and PI-3 is the most rigid, because a more flexible polymer has a lower characteristic ratio. This result is consistent with the result of conformational analysis. The limiting characteristic ratios, 7–9, for these polyimides are comparable to that of other polyimides[13], namely 6.43.

Mechanical properties

The cohesive energy density of a polymer in the bulk is sometimes used as a rough indicator of a mechanical property of the polymer. Generally larger cohesive density results in larger elastic modulus. In an atomistic modelling, the cohesive energy, E_{coh}, is defined as the increase in energy per mole of a polymer if all intermolecular forces are removed. Thus the cohesive energy can be calculated by the difference in the potential energies between the isolated chain and the parent chain in the bulk, i.e.

$$E_{coh} = E_{isolated} - E_{bulk}. \tag{8}$$

The Hildebrand solubility parameter, δ, is defined as the square root of the cohesive energy density, E_{coh}/V, where V is the volume of an amorphous cell. *Table 8* lists the simulated solubility parameters of the four polyimides. These values, 9.56–11.42, are comparable with the value, ~11.3 $(kcal/mol)^{1/2}$, of other polyimides calculated from simulation[12]. Here, PI-2 has the lowest value of solubility parameter and PI-3 has the highest value, which is the same trend as observed in the characteristic ratio. This indicates that a more flexible chain has a lower solubility parameter. This is easily understood by considering that a more flexible chain results in loose packing in the bulk, thereby yielding a lower cohesive density. This cohesive energy density or solubility parameter can then be related to the mechanical properties such as modulus and yield behaviour, as will be discussed later.

Elastic constants can be calculated from changes in the total energy of the systems subjected to deformation. After an initial energy minimization, a very small strain (0.05%) is applied to the system and then a second energy minimization is performed. By definition, the first derivative of the potential energy with respect to strain is the internal stress tensor and the second derivative represents the stiffness matrix. Thus, the stiffness matrix, C_{ij}, is given by

$$C_{ij} = (\partial^2 U/\partial\epsilon_i\partial\epsilon_j)/V = \partial\sigma_i/\partial\epsilon_j = (\sigma_{i+} - \sigma_{i-})/(2\epsilon_j) \tag{9}$$

where σ_i and ϵ_i are the ith components of the stress and strain tensors, and σ_{i+} and σ_{i-} are stress components under tension and compression, respectively. The stiffness matrices calculated by averaging six model structures for each polyimide are shown in equations (10a), (10b), (10c) and (10d). A more detailed procedure[7] for calculating the stiffness matrix is described elsewhere.

$$\begin{pmatrix} 6.69 & 2.55 & 2.79 & -0.21 & -0.32 & 0.09 \\ 3.18 & 6.26 & 2.98 & 0.43 & -0.38 & -0.18 \\ 2.89 & 3.39 & 6.57 & 0.54 & 0.12 & -0.35 \\ 0.67 & 0.51 & 0.42 & 1.47 & 0.15 & 0.43 \\ -0.11 & -0.28 & -0.48 & 0.81 & 2.11 & 0.34 \\ 0.19 & -0.04 & -0.73 & -0.23 & -0.62 & 1.77 \end{pmatrix}$$

for PI − 1 (10a)

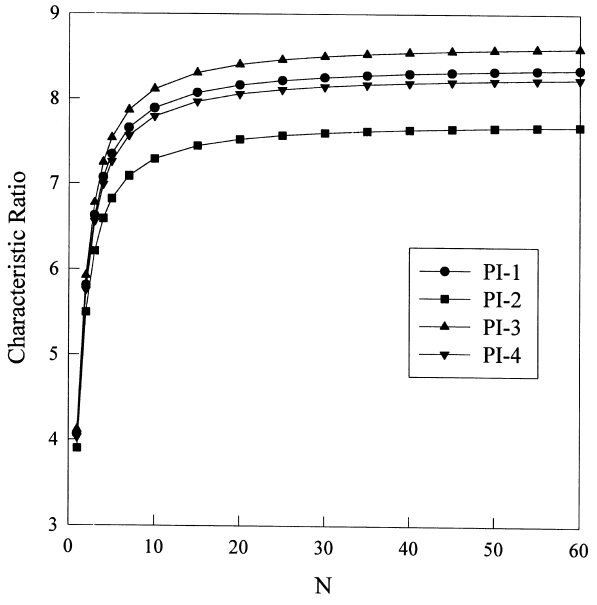

Figure 5 Characteristic ratios of four polyimides calculated as a function of *N*, the number of repeating units

Table 8 Solubility parameters of the model polyimides from simulation

Polymers	PI-1	PI-2	PI-3	PI-4
Solubility parameter $((cal/cm^3)^{1/2})$	10.91 ± 0.18	9.56 ± 0.39	11.42 ± 0.24	10.75 ± 0.28

$$\begin{pmatrix} 5.03 & 2.33 & 2.24 & 0.38 & 0.26 & -0.30 \\ 2.46 & 5.20 & 2.89 & 0.63 & -0.32 & 0.58 \\ 2.25 & 1.91 & 6.05 & -0.45 & 0.08 & 0.21 \\ -0.49 & -0.67 & 0.47 & 1.77 & 0.59 & -0.42 \\ -0.57 & -0.12 & -0.26 & -0.15 & 1.36 & -0.61 \\ -0.70 & 0.33 & -0.29 & 0.11 & -0.50 & 1.48 \end{pmatrix}$$

for PI – 2 (10b)

$$\begin{pmatrix} 8.21 & 3.67 & 4.01 & 0.55 & 0.33 & -0.17 \\ 4.38 & 8.93 & 3.71 & -0.39 & -0.14 & -0.08 \\ 3.49 & 3.09 & 7.05 & 0.66 & 0.22 & 0.36 \\ -0.52 & -0.19 & -0.40 & 2.11 & -0.23 & 0.41 \\ -0.15 & 0.54 & 0.63 & 0.18 & 2.56 & 0.30 \\ -0.68 & 0.23 & 0.48 & -0.34 & 0.25 & 1.63 \end{pmatrix}$$

for PI – 3 (10c)

$$\begin{pmatrix} 5.51 & 2.08 & 1.92 & -0.62 & -0.53 & 0.30 \\ 2.79 & 6.17 & 3.54 & 0.54 & -0.19 & -0.22 \\ 2.13 & 3.56 & 6.38 & -0.32 & 0.47 & -0.43 \\ 0.05 & -0.13 & 0.38 & 1.25 & -0.46 & 0.08 \\ 0.27 & -0.65 & 0.35 & 0.39 & 1.69 & -0.50 \\ -0.37 & 0.13 & -0.14 & -0.26 & 0.51 & 2.14 \end{pmatrix}$$

for PI – 4 (10d)

For isotropic amorphous material, the stiffness matrix should always be symmetric, and thus has the following form:

$$\begin{pmatrix} \lambda+2\mu & \lambda & \lambda & 0 & 0 & 0 \\ \lambda & \lambda+2\mu & \lambda & 0 & 0 & 0 \\ \lambda & \lambda & \lambda+2\mu & 0 & 0 & 0 \\ 0 & 0 & 0 & \mu & 0 & 0 \\ 0 & 0 & 0 & 0 & \mu & 0 \\ 0 & 0 & 0 & 0 & 0 & \mu \end{pmatrix} \quad (11)$$

where λ and μ are Lame's constants. The stiffness matrices calculated from simulation show a slight deviation from the idealistic case, since the actual calculation of C_{ij} and C_{ji} follows two different deformation paths. Nevertheless, the calculated stiffness matrices still show the basic features of an isotropic polymer. The Lame constants for the model structures can be calculated from the following relation:

$$\lambda = \frac{1}{3}(C_{11}+C_{22}+C_{33}) - \frac{2}{3}(C_{44}+C_{55}+C_{66}) \quad (12)$$

$$\mu = \frac{1}{3}(C_{44}+C_{55}+C_{66}).$$

The Young's modulus E, shear modulus G, bulk modulus B, and Poisson ratio ν are related with the Lame constants as follows:

$$E = \mu\frac{3\lambda+2\mu}{\lambda+\mu} \qquad G = \mu$$
$$B = \lambda + \frac{2}{3}\mu \qquad \nu = \frac{\lambda}{2(\lambda+\mu)}. \quad (13)$$

The calculated properties and experimental Young's moduli are listed in *Table 9*. The simulated Young's moduli agree well with the experimental data[11,15,16] considering the possible existence of microscopic or macroscopic defects in the experimental sample and the difference in the magnitude of applied strain between simulation and experiment. It is more interesting to note that the order of values of Young's moduli calculated from simulation is exactly the same as the experimental one, i.e. the magnitudes of Young's moduli are in the order of PI-3 > PI-1 > PI-4 > PI-2. It is very clear that the mechanical properties are closely related to the chain flexibility, when the results of *Table 9* are compared with those of *Figure 5*. In other words, a more flexible polyimide has a lower Young's modulus. The modulus is also related to the solubility parameter (*Table 7*) as mentioned earlier in this section: the larger the solubility parameter, the higher the modulus.

There are two methods to obtain a stress–strain curve from atomistic modelling techniques. One is the use of a molecular mechanics technique and the other is the use of a molecular dynamics technique. In the first method, the strain is applied by changing the cell parameters—for example, if we want to apply a strain, ϵ_{33}, then we will increase the value of the cell parameter c—and then the other cell parameters as well as the coordinates are optimized by the molecular mechanics technique. The stress, σ_{33}, is then obtained from the corresponding component of the internal stress tensor. In this method, the variation of properties with time cannot be observed, because molecular motions are not considered in molecular mechanics. Nevertheless, it is known that molecular mechanics yields a value closer to the experimental one than molecular dynamics[17]. In the second method, a stress–strain curve is obtained from a

Table 9 Mechanical properties for the model polyimides

Polymers	Mechanical properties				
	Young's modulus, GPa	Bulk modulus, GPa	Compressibility, GPa^{-1}	Shear modulus, GPa	Poisson's ratio
PI-1	4.67 ± 0.43 (3.72)[a]	4.14 ± 0.89	0.24 ± 0.09	1.78 ± 0.59	0.31 ± 0.05
PI-2	4.01 ± 0.68 (3.33)[b]	3.37 ± 0.60	0.29 ± 0.11	1.54 ± 0.52	0.30 ± 0.04
PI-3	5.56 ± 0.65 (4.96)[a]	5.26 ± 1.27	0.19 ± 0.07	2.10 ± 0.60	0.32 ± 0.04
PI-4	4.41 ± 0.51 (3.50)[b]	3.76 ± 0.61	0.27 ± 0.06	1.69 ± 0.65	0.30 ± 0.05

[a]The values in parenthesis represent experimental data taken from [16]
[b]The values in parenthesis represent experimental data taken from [11]

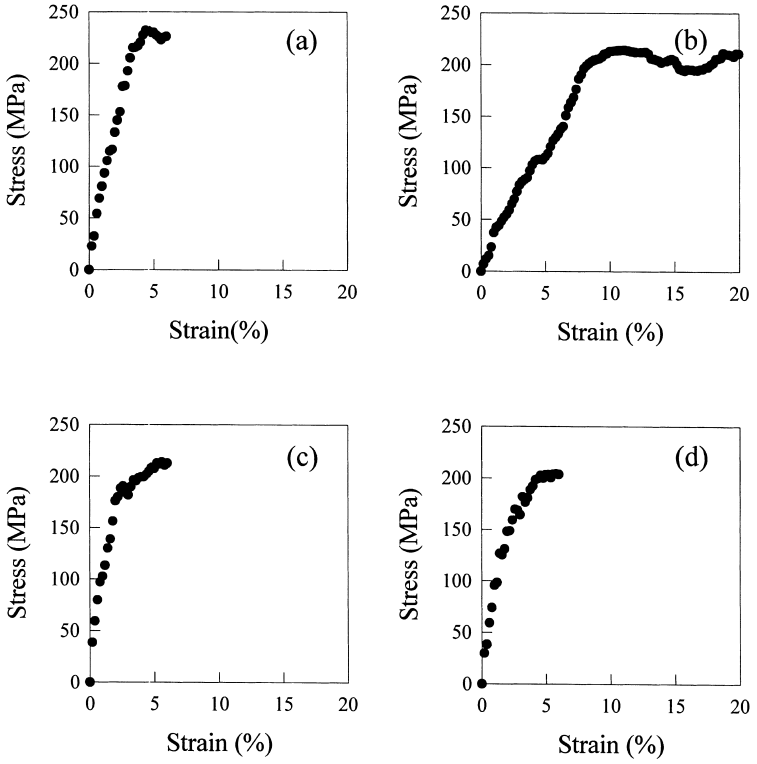

Figure 6 Averaged stress–strain curves of four model polyimides: (a) PI-1, (b) PI-2, (c) PI-3, and (d) PI-4

constant-stress molecular dynamics simulation. But this method has some limitations: the method usually gives a very large value of modulus because the strain rate for simulation is very fast compared with experimental ones. Moreover, this method is a very time-consuming procedure, and fluctuations of the strain with time are usually very large. Therefore, the first method was adopted for our simulation, because the variation of properties with time is not pursued in this study.

Each stress–strain curve was generated with a strain of 0.2% up to 6% except PI-2 (in this case up to 25%). For each model structure, three stress–strain curves are obtained representing measurements in three independent directions, *x*, *y* and *z*. As a result, a total of 18 stress–strain curves were generated for each polyimide, and then averaged. The averaged stress–strain curves of the four polyimides are shown in *Figure 6*. All the polyimides show yielding behaviour. The yield stresses and strains calculated from simulations are listed in *Table 10* and compared with experimental data. The yield stresses from simulation are larger than the experimental values. This discrepancy may come from several sources, the primary one, most probably, being the small size of the simulation box. Moreover, the

Table 10 Yield strains and stresses of the model polyimides

Polymers	Yield strain (%)		Yield stress (MPa)	
	Simulation	Experiment	Simulation	Experiment
PI-1	3.6 ± 0.5	3.0[a]	216 ± 21	120[a]
PI-2	11.0 ± 0.9	12.2[b]	214 ± 35	130[b]
PI-3	2.5 ± 0.5	1.13[c]	190 ± 23	75[c]
PI-4	4.2 ± 0.6	—[d]	198 ± 27	—[d]

[a]Taken from [15]
[b]Taken from [11]
[c]Elongation at break and breaking stress before it shows yielding taken from [15]
[d]Not available

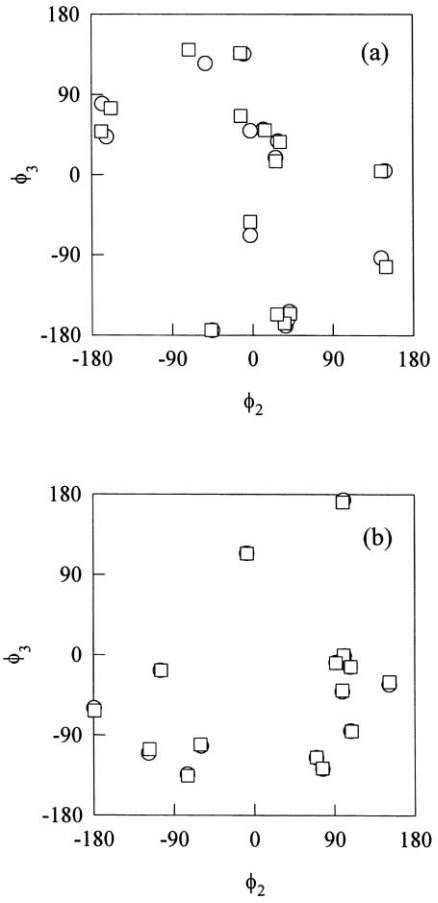

Figure 7 Torsional angle distributions of (a) PI-2 and (b) PI-3 before and after deformation. The symbols (○) and (□) represent before and after deformation (2.0%), respectively

energy minimization by the molecular mechanics technique assumes no thermal motion; therefore, it simulates the property of a material near 0 K, whereas the experimental values in *Table 10* were measured at room temperature. Thus the comparison of results from the molecular mechanics simulation with experimental ones should be made by extrapolating the experimental data to 0 K, which are not available at the present time. Nevertheless, the yield strains from simulation agree well with experimental ones. The simulated stress–strain curve of PI-3 shows yield behaviour, although the experimental data do not show the yielding. As mentioned in the previous section, the PI-3 chain is very rigid and thus its chain mobility will be very low. Consequently, the chain may not easily move to the new stable conformational state corresponding to the applied strain. As a result, the material becomes broken even at a small strain. However, in the molecular mechanics simulation the chain can move to the new set of positions corresponding to the applied strain because this technique provides enough mobility to lower the potential energy. Therefore, the molecular mechanics simulation will always show the yield behaviour regardless of the chain rigidity.

It has been reported that the nature of yielding is due to the characteristics of the Lennard–Jones potential if the van der Waals interactions are dominant in the deformation[18]. However, it is informative to examine the change in torsional angle distributions during deformation. *Figure 7* compares torsional angle distributions of PI-2 and PI-3 before and after deformation. The more flexible polyimide PI-2 shows a significant difference in torsional angle distributions before and after deformation (2.0%), while the more rigid PI-3 does not show a discernible change in torsional angle distributions. In other words, the more flexible PI-2 chain has more degrees of conformational freedom as compared with the more rigid PI-3 during deformation. It is interesting to note that the polyimide with more degrees of conformational freedom shows the larger yield strain, although the mechanism by which the chain flexibility affects the van der Waals energy is not clearly understood at this time.

CONCLUSIONS

An atomistic modelling technique has been successfully applied to four polyimides, BTDA-CDA, BTDA-ODA, BTDA-SDA and BTDA-MDA, to develop some structure–property relationships. The only difference in chemical structure between the four polyimides is the linkage atom of diphenyls in the diamine moiety. Chain flexibility was evaluated by analysing conformational contour maps and by calculating characteristic ratios. Elastic moduli were calculated from the stiffness matrix simulated by molecular mechanics, and the stress–strain curves were also obtained by energy minimization. The polyimide PI-2 with an oxygen linkage was the most flexible whereas the polyimide PI-3 with a sulfonyl linkage was the most rigid. A more flexible polyimide has higher degree of conformational state, smaller characteristic ratio, lower solubility parameter, lower elastic modulus and larger yield strain.

REFERENCES

1. Theodorou, D. N. and Suter, U. W., *Macromolecules*, 1985, **18**, 1467.
2. Theodorou, D. N. and Suter, U. W., *Macromolecules*, 1986, **19**, 139.
3. Boyd, R. H. and Pant, P. V. K., *Macromolecules*, 1991, **24**, 4078.
4. Fan, C. F. and Hsu, S. L., *Macromolecules*, 1992, **25**, 266.
5. Raaska, T., Niemela, S. and Sundholm, F., *Macromolecules*, 1994, **27**, 5751.
6. Hutnik, M., Argon, A. S. and Suter, U. W., *Macromolecules*, 1993, **26**, 1097.
7. Fan, C. F., Cagin, T., Chen, Z. M. and Smith, K. A., *Macromolecules*, 1994, **27**, 2383.
8. Vasudevan, V. J. and McGrath, J. E., *Macromolecules*, 1996, **29**, 637.
9. Fan, C. F. and Hsu, S. L., *Macromolecules*, 1991, **24**, 6244.
10. Mayo, S. L., Olafson, B. D. and Goddard, W. A., *J. Phys. Chem.*, 1990, **94**, 8897.
11. Bessonov, M. I., Koton, M. M., Kudryavtsev, V. V. and Laius, L. A., *Polyimides: Thermally Stable Polymers*. Consultants Bureau, New York, 1987.
12. Zhang, R. and Mattice, W. L., *Macromolecules*, 1995, **28**, 7454.
13. Zhang, R. and Mattice, W. L., *Macromolecules*, 1993, **26**, 6100.
14. Mattice, W. L. and Suter, U. W., *Conformational Theory of Macromolecules, The Rotational Isomeric State Model in Macromolecular Systems*. Wiley, New York, 1994.
15. Mittal, K. L. (ed.), *Polyimides: Synthesis, Characterization and Application*, Vol. 1. Plenum Press, New York, 1982.
16. Wilson, D., Stenzenberger, H. D. and Hergenrother, P. M. (eds.), *Polyimides*. Blackie and Son, Glasgow, 1990.
17. Cahn, R. W., Haasen, P. and Krammer, E. J. (eds.), *Materials Science and Technology*, Vol 12. VCH, Weinheim, 1993, p. 33.
18. Fan, C. F., *Macromolecules*, 1995, **28**, 5215.